Effect of Heat Treatment Conditions on Retained Austenite and Corrosion Resistance of the X190CrVMo20-4-1 Stainless Steel

Effect of Heat Treatment Conditions on Retained Austenite and Corrosion Resistance of the X190CrVMo20-4-1 Stainless Steel

M. C. Bignozzi[1], L. Calcinelli[1], M. Carati[2], L. Ceschini[1], C. Chiavari[3], G. Masi[1], A. Morri[4*]

[1] Department of Civil, Chemical, Environmental and Materials Engineering (DICAM), University of Bologna, via Terracini 28, 40136 Bologna, Italy
[2] Closures, Containers & PET Division, SACMI IMOLA S.C., Via Selice Provinciale, 17/A, 40026 Imola, BO, Italy
[3] Department of Cultural Heritage (D.B.C.), University of Bologna, via degli Ariani 1, 48121 Ravenna, Italy
[4] Department of Industrial Engineering (DIN), University of Bologna, viale del Risorgimento 4, 40136 Bologna, Italy

Abstract

In the present work the microstructural characterization of the powder-metallurgy X190CrVMo20-4-1 has been performed and correlated with its corrosion properties. The martensitic stainless steel was hardened at different austenitizing and tempering temperatures. Microstructural analyses were carried out using Scanning Electron Microscopy (SEM–EDS) to define the carbide distribution in the steel matrix. Carbides morphology and retained austenite content were evaluated and correlated to the corrosion behaviour of the different heat-treated steels, investigated by means of electrochemical tests. The results show the presence of $M_{23}C_6$ and M_7C_3 Cr-V based carbides homogenously dispersed in the matrix in annealed and quenching-and-tempering conditions. The carbides dissolution was evaluated by image analysis in every different heat treatment condition. When low tempering temperature was applied, an increasing in retained austenite content was defined by high austenitizing temperature and elevated carbides solubilization. At high tempering temperature, retained austenite content was not up to 5% nor affected by austenitizing temperature. Contrary to the expectations, HRC hardness was not influenced by the heat treatment conditions and retained austenite content. Corrosion resistance of the different heat-treated samples was found to be mainly influenced by retained austenite volume fraction and the tempering temperature. In particular, high austenitizing temperature and low tempering temperatures allowed the best corrosion resistance among the different heat treatment parameters investigated. The results obtained in the experimentation can provide support to the heat treatment optimization of the steel, widely used in tool and mould applications.

Keywords Tool steel, Quenching and tempering, Carbides, Retained austenite, Corrosion, Current density-potential curve

1 Introduction

Martensitic stainless steels are high-carbon and high-chromium ferrous alloys widely used in many industrial applications because of their high strength, high hardness and wear resistance, combined with a good corrosion resistance. These properties, however, are significantly affected by the manufacturing technology and the heat treatment conditions, strictly related to their chemical composition. Among different applications, martensitic stainless steels are also widely used as plastic mould materials, and proper com- position and production techniques have been developed to satisfy the needs of the plastic processing industry. Among the wide availability of tool steels, the high-alloyed X190CrVMo20-4-1 is a martensitic chromium steel produced by powder metallurgy (PM) that due to the high alloying content offers extremely high wear resistance and good corrosion resistance. This producing process is widely used in the production of highly alloyed tool steel, to enhance cleanliness and purity by reducing inclusion and segregation. In fact, these steels under conventional casting process are generally associated with slow cooling rates, resulting in the formation of coarse carbides and macro segregation, hard to be broken during hot working. Instead, the PM process reduces non-metallic inclusions, segregation and guarantees a microstructure finer than conventionally steel with a consequent improvement of the microstructural features and, consequently, the mechanical properties [1,2]. High amounts of alloying elements in tool steel are necessary to improve their mechanical and corrosion behaviour. In the X190CrVMo20-4-1 steel, high carbon, chromium, molybdenum and vanadium content allows obtaining, after quenching and tempering (Q&T), a martensitic matrix microstructure with Cr-V carbides, which improve hardness and wear resistance [3–5]. Moreover, chromium content over 12%, guarantees the formation of a passive Cr film, which protect from corrosive agents. Nevertheless, the high alloying element content significantly influences the heat treatment response. High carbon content lowers the martensite start and finish temperatures (M_S and M_f) and this can lead to a high content of retained austenite (RA) after quenching [2,6]. The softer retained austenite (RA) is generally an undesired phase because it degrades hardness, fatigue and wear resistance. RA also negatively affects the dimensional stability of the heat-treated parts [1], that is of fundamental

importance in mould steel, since is a metastable phase which can be transformed into martensite and secondary carbides under either stress [7] or sub-zero temperature holdings [8,9]. In many papers a volumetric expansion phenomenon, related with the lattice distortion, has been observed due to the RA decomposition under local stresses [10–12]. In the Q&T condition, the variables that mainly affect the final properties of the X190CrVMo20-4-1 are the austenitizing temperature (T_{aus}), possible cryogenic treatment and tempering temperature (T_{temp}). The austenitizing temperature has a large influence on the dissolution rate of carbides, which severally affects the amount of alloying elements in the austenite and consequently M_S and M_f temperatures [13,14]. Indeed, as reported in many studies [4,15,16], lowering the austenitizing temperature a lesser content of carbon and alloying elements solubilizes from primary carbides and, consequently, a lower percentage of RA is present in the steel after quenching. RA, however, can be partially or completely eliminated by: (1) cryogenic treatment or (2) high tempering temperature. Cryogenic treatments are widely used to promote the complete transformation of RA in martensite during quenching, improving hardness and wear resistance [8,17]. When cryogenic treatments are carried out until − 120 °C, the enhancement of wear resistance is attributed to the transformation of RA and also to both car- bides refinement and their more homogeneous distribution [8,17,18]. When a deep cryogenic treatment at − 196 °C is carried out, the hardness is not strongly affected [18] and the enhancement in wear resistance is mostly attributed to the carbide refinement and eventually to the precipitation of a fine η-carbides [19]. Tempering also notoriously affects the final microstructure of Q&T tool steels: low tempering temperatures (200–300 °C) can be applied to relieve the martensite and decrease internal stress. Moreover, the formation of Fe_2C is promoted which can transform to Fe_3C with tempering above 300 °C. When tempering temperature is over 400–450 °C [11,12], RA is transformed into martensite and secondary carbides with a corresponding secondary hardness peak [5,20]. However, as reported in [21,22] at the high tempering temperature the precipitation of nano-sized Cr-rich MC, M_2C and $M_{23}C_6$ carbides leads to Cr-depleted zones close to the precipitates boundary and consequently the corrosion resistance can dramatically deteriorate. Corrosion resistance is an important property for highly alloyed martensitic stainless steels and it is mainly related to the alloying elements and its microstructure. In particular, the amount of chromium in the steel matrix (usually higher than 12%), the carbide volume fraction precipitated in the steel matrix and the amount of RA are the main parameters that can affect the corrosion behaviour. In addition, the processing route [23] and the heat treatment strongly influence the corrosion behaviour as reported in many studies [22–24]. So, corrosion resistance is mainly related to the carbide volume fraction dissolved in the matrix after austenitizing during quenching and is sensitive to the carbide precipitation during tempering [24]. In particular, increasing T_{aust} usually leads to an improvement in corrosion resistance [24,25] mainly due to the increase of solved Cr-rich carbides into the matrix. It was found that the breakdown potential tends to increase with increasing T_{aust} while passive current density decreases, indicating an improvement in resistance opposed by the material to initiation of localized corrosion [25]. However, Candelaria et al. [24] highlight that in the range of T_{aust} between 1050 and 1075 °C corrosion resistance unexpectedly decreases, while for higher temperatures up to 1100 °C corrosion resistance is recovered. The behaviour recorded in the range of 1050–1075 °C is explained as a consequence of the increase of the internal martensite lattice stresses that are promoted by the increase of carbon saturation when T_{aust} is raised. Conversely, at T_{aust} = 1100 °C the RA volume fraction increases leading to a beneficial influence on corrosion behaviour, due to the decrease of the internal stresses [24–26]. So, the RA amount increases when T_{aust} is raised due to the fact that primary carbides dissolution is favoured with a consequent increase of C and other alloying elements in the steel matrix. Thereby, the austenite stability is enhanced, resulting in a higher amount of austenite that can- not complete the austenite/martensite transformation [27]. Many studies have investigated the effect of tempering on the corrosion behaviour of this kind of steels [22, 26, 28, 29] due to the fact that tempering is useful to reduce the stresses, modify carbides precipitation, transform RA into martensite, so as to control the corrosion rate by appropriate processing conditions. High T_{temp} (450–560 °C) close to the secondary hardness peak is detrimental for corrosion resistance due to the formation of tempering carbides that lead to a Cr depletion in the steel matrix, increase of boundaries between Cr- rich carbides and the matrix or weakening of the oxide layer [22,26,28,29]. For this reason, tempering at low temperature should be favoured as corrosion resistance is improved due to the decrease of internal stresses [22,26,28]. Based on the above, the proper selection of heat treatment parameters plays a key role in defining the final mechanical and corrosion behaviour of highly alloyed martensitic stain- less steels and, for this reason, the aim of this paper was to investigate the effect of quenching and tempering conditions on the microstructure and, consequently, on the corrosion resistance on the innovative X190CrVMo20-4-1 martensitic stainless steel produced by PM.

2 Materials and Methods

The present study was carried out on the X190CrVMo20-4-1 tool steel produced by powder metallurgy (PM). In the innovative manufacturing process, the powder is melted, atomized and then hot isostatic pressed (HIP) into billets conventionally forged or rolled into bars. The chemical composition was checked with a Glow-Dis- charge Optical Emission Spectroscope (GDOES) Spectruma Analytik GDA650, and the results are reported in Table 1.

Table 1 Chemical composition (wt%) of the X190CrVMo20-4-1 martensitic stainless steel

Element	C	Mn	Si	Cr	Ni	Mo	V	W	Fe
Average	1.96	0.21	0.58	19.43	0.36	1.0	4.88	0.48	70.53
SD	0.01	0.01	0.01	0.03	0.01	0.01	0.01	0.01	0.01

Disks (Ø50 × 3 mm) obtained from an annealed bar were heat treated in a vacuum furnace at different austenitizing and tempering temperatures, as reported in Table 2; they were quenched under the same conditions, using Nitrogen at a pressure of 10 bar. Austenitizing and tempering temperatures are confidential data and have been reported in ranges. High austenitizing temperature means higher than 1120 °C, medium is between 1120 and 1100 °C and low means lower than 1100 °C. High tempering temperature means higher than 450 °C, and low is lower than 350 °C. Holding times are confidential too, however they were kept constant for all the performed heat treatments. Different austenitizing and tempering temperatures were applied with the principal aim of investigating their effect on the amount of retained austenite and consequently on both hardness and corrosion resistance. The austenitizing time was not considered in this study, but as reported in [30] the rate of diffusion processes is mainly influenced by temperature than by time.

Table 2 Summary of austenitizing and tempering conditions. Three tempering cycles were carried out for each heat treatment cycle

Sample	Austenitizing temperature (°C)	Tempering temperature (°C)
HA-HT	High (> 1120)	High (> 450)
HA-LT	High (> 1120)	Low (< 350)
MA-LT	Medium (1100–1120)	Low (< 350)
LA-LT	Low (< 1100)	Low (< 350)

X-ray diffraction analysis (XRD) was carried out with a X-ray diffractometer with Co-Kα radiation (Kα1 = 1.78901 Å, 35 kV, 30 mA), and a Fe filter for sup- pressing Kβ radiation (PW1729 X-ray generator—Philips). Calibration was performed by means of Cu radiation (Kα1 = 1.5405 Å, 0.005 2θ/s, 10 s), using Si as standard reference material (Ref. 00-027-1402 quality star(S)). A 2θ angle in the range 55° to 105° was selected, with a scanning speed of 0.5 2θ/min. From the XRD diagrams the volume content of retained austenite (RA) was measured using ASTM E975 standard [31]. Hardness was measured with a Rockwell tester Officine Galileo A200, and a load of 150 kg (HRC), according to EN ISO 6508 [32]. Microstructural analyses were carried out on metallographic samples either in the annealed and Q&T conditions (reported in Table 2). They were mechanically ground with emery papers then polished with 1 μm diamond paste and finally chemical etched with Vilella's reagent (5 cc HCl + 1 g picric acid + 100 cc ethyl alcohol). The microstructures were observed with a scanning electron microscope (SEM) Carl Zeiss EVO50, equipped with an Oxford Instrument INCA X-Act PentaFet Precision energy dispersive spectroscope (EDS). The working voltage of both SEM and EDS was 20 kV, while the current was 100 pA and 500 pA for SEM and EDS respectively. Analysis of the carbides was carried out on annealed and Q&T samples, polished and etched with Murakami's reagent (100 ml H_20 + 10 g KOH + 10 g $K_3Fe(CN)_6$). The estimation of the carbides parameters was made according to ASTM A892-09 [33] and many studies [8, 34], with the help of Image-J image analysis software, using several random SEM images at the same magnification. Total amount of carbides and mean population density for average size were analysed. The total amount of car- bides present in every sample was estimate as percentage of the total area occupied. For the evaluation of the mean population density, carbides were classified by average size (< 1 μm^2; 1–2 μm^2; 2–3 μm^2; 3–4 μm^2; > 4 μm^2). The number of carbides considered for the analysis was a minimum of 3000 for each sample, to evaluate the statistical reliability associated with the measurement. The chemical composition of carbides was analysed by SEM–EDS. Polarization curves were recorded at a constant temperature of 30 °C using 0.1 M sulphuric acid (H_2SO_4) solution as electrolytic solution, in order to characterize the active/ passive

behaviour of the heat-treated X190CrVMo20-4-1 samples and evaluate which heat treatment lead to a better corrosion resistance in presence of aggressive environment. The set up of the electrochemical test was the conventional three-electrodes cell in which heat-treated sample acted as the working electrode (WE), a platinum electrode as the counter electrode (CE) and a saturated calomel electrode (SCE) as the reference electrode (RE). The anodic polarization curves were obtained by using an electrochemistry potenziostat (Amel, model 7050, Italy) and were recorded starting 0.1 V lower than the open circuit potential (OCP) up to 1.5 V higher than the OCP. This potential range was selected in accordance with the available literature [22,23,28]. A scan rate of 0.166 mV s^{-1} was applied in accordance with ASTM G5-14 [35]. To ensure a comparable initial state for all the samples, a measurement of OCP was carried out for 10 min before the test. Polarization curves were repeated for each sample in order to ensure reproducibility of the results. As sample preparation, the heat-treated specimens were connected from the backside with a braze-welded coated copper wire. Subsequently they were embedded in a methyl-methacrylate resin and all the specimens were ground using abrasive SiC paper up to 1000 grit. In this way, the free surface area exposed to the electrolytic solution of each sample was of 2.27 cm^2.

3 Results

3.1 Microstructure Analysis

The microstructure of the annealed bar consists of homogeneously distributed and very fine (mostly < 1–1.5 μm) Cr-V carbides, as shown by SEM–EDS analyses reported in Fig. 1a, b. The EDS analysis demonstrates that, despite the large amount of Mo, all the carbides visible with SEM microscope, are Cr-V rich, independently by their size, as shown by a representative EDS spectrum (Fig. 1c). Size and homogeneous distribution of the car- bides, as well as negligible amount of non-metallic inclusions are peculiarity of the highly controlled PM production process of this steel. Representative SEM micrographs of the steel after the different tested quenching and tempering conditions are reported in Fig. 2a–h. In particular, Fig. 2a, b shows micro- structures of samples austenitized at high temperature and tempered at high temperature (HA-HT samples), while in Fig. 2c, d the typical microstructures of samples subjected to low tempering temperature (HA-LT samples) are reported. A full martensitic matrix, with its typical acicular morphology, was observed in the samples austenitized and tempered at high temperature (HA-HT) (Fig. 2a,b); while microstructure of the samples austenitized at high temperature and tempered at low temperature (HA-LT) consisted of a martensitic matrix were large smooth zones with retained austenite were alternated (Fig. 2c,d). Samples austenitized at medium temperature and tempered at low temperature (MA-LT) were characterized, by a martensitic matrix interrupted by small smooth plates in correspondence of the retained austenite (Fig. 2e,f), while samples treated at the lower austenitizing temperature and same tempering temperature (LA-LT), displayed an almost completely martensitic microstructure (Fig. 2g,h). It is well known that carbides distribution, size and morphology play a dominant role on the mechanical properties of tool steels and for this reason their evaluation is an important step of steel quality evaluation. Q&T led to a considerable modification in the size and amount of the primary carbides with respect to the annealed condition, as highlighted by the results of the image analysis reported in Figs. 3 and 4. In particular, Fig. 3 shows the amount of carbides, evaluated as percentage of area, while Fig. 4 displays the carbides distribution for average size. It can be clearly seen that different Q&T conditions induce, with respect to the annealed bar, a reduction in the amount of primary carbides (Fig. 3). In fact, while the per- centage of carbides in the annealed bar is about 20%, after Q&T it is reduced between 15 and 17% due to the solubilization of carbides during the heat treatment. It is well known, in fact, that austenite has a high solubility limit for carbon and alloying elements, and some carbides will therefore dissolve into the matrix during the austenitizing phase of the heat treatment. As shown in Fig. 4, high austenitizing temperatures lead to a solubilization of about the 75.5% of the smaller carbides (< 1 μm^2 area) and 12.2% of the larger carbides (> 4 μm^2), while low austenitizing temperature solubilized only the 43.3% and 22.1% of the smaller and large carbides, respectively. Secondary carbides, were not resolvable by SEM analyses because of their nanometric size [21,36].

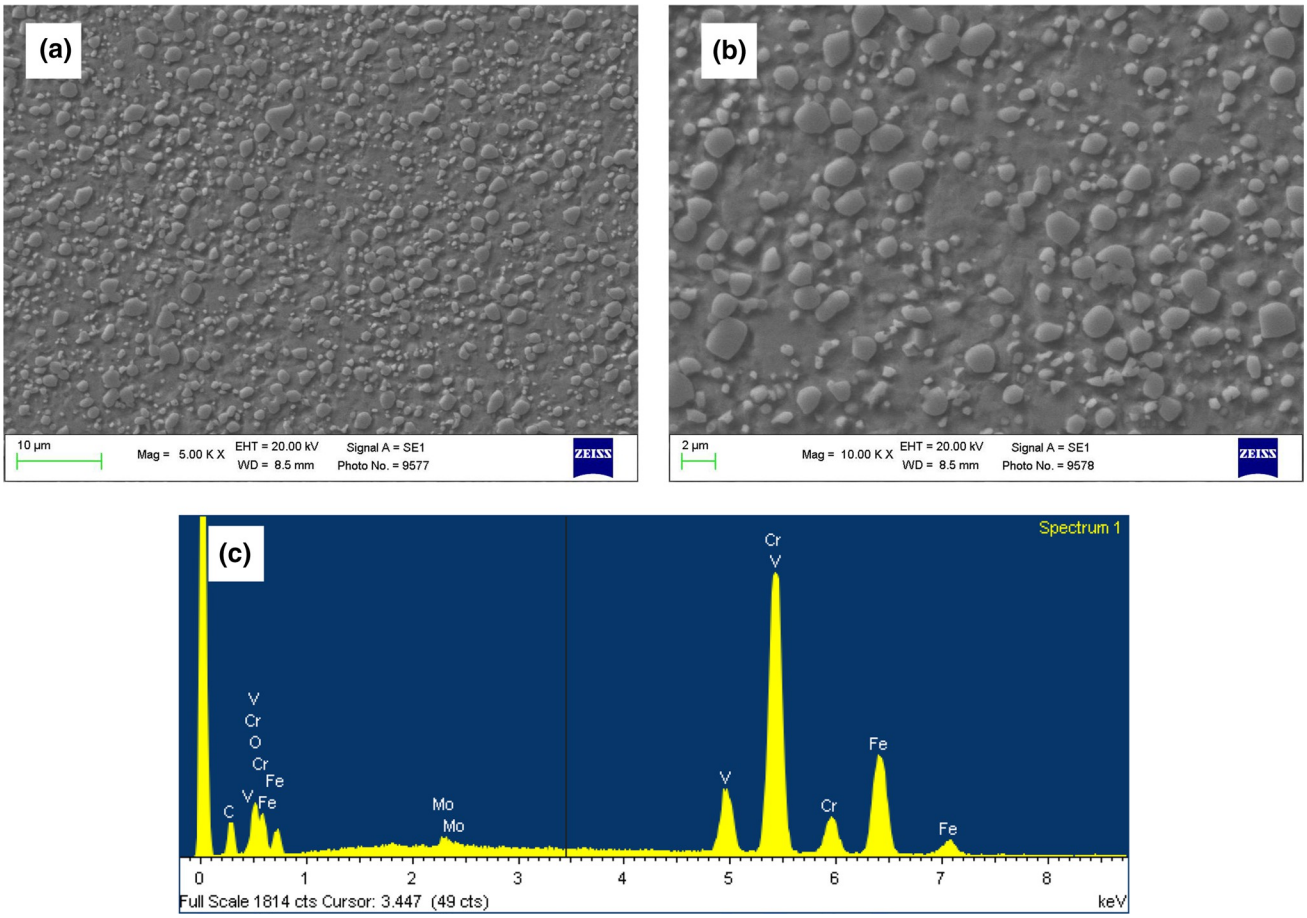

Fig. 1 SEM micrographs, ×5000 (**a**) and ×10,000 (**b**) of the annealed sample; a representative EDS spectrum of primary Cr-V carbides (**c**)

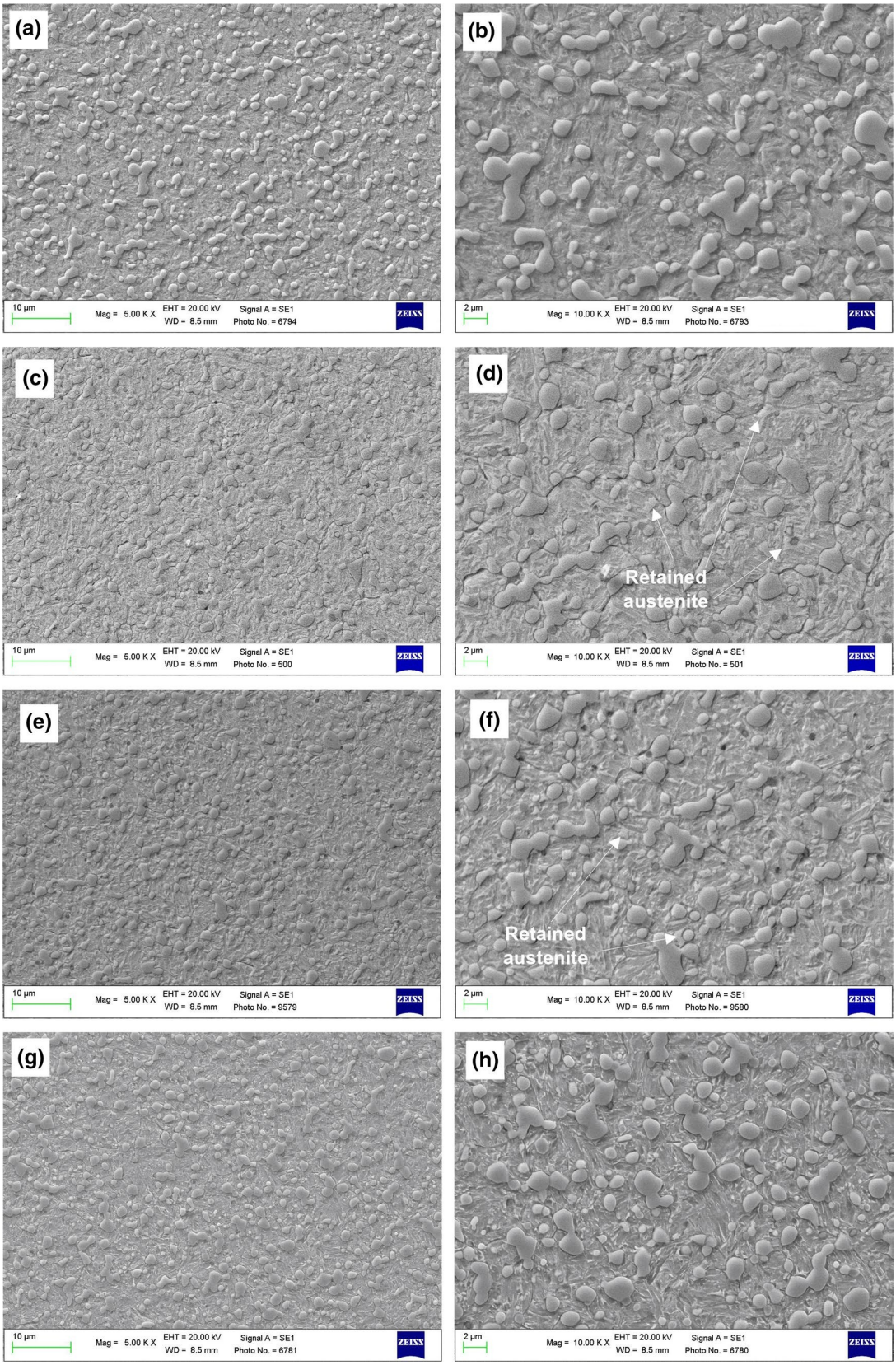

Fig. 2 SEM micrographs of: sample HA-HT, ×5000 and ×10,000 (**a**, **b**); sample HA-LT, ×5000 and ×10,000 (**c**, **d**); sample MA-LT, ×5000 and ×10,000 (**e**, **f**); sample LA-LT, ×5000 and ×10,000 (**g**, **h**)

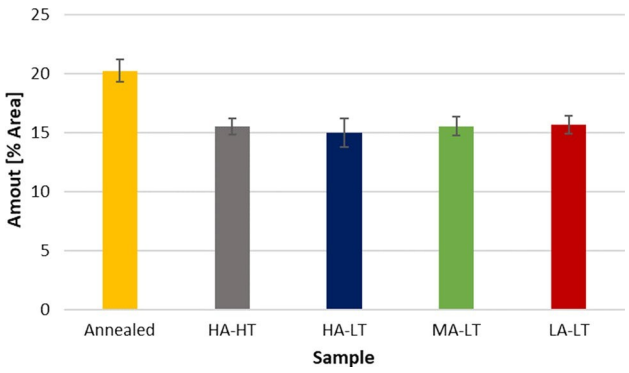

Fig. 3 Amount (as area%) of primary carbides present in annealed and different Q&T condition samples

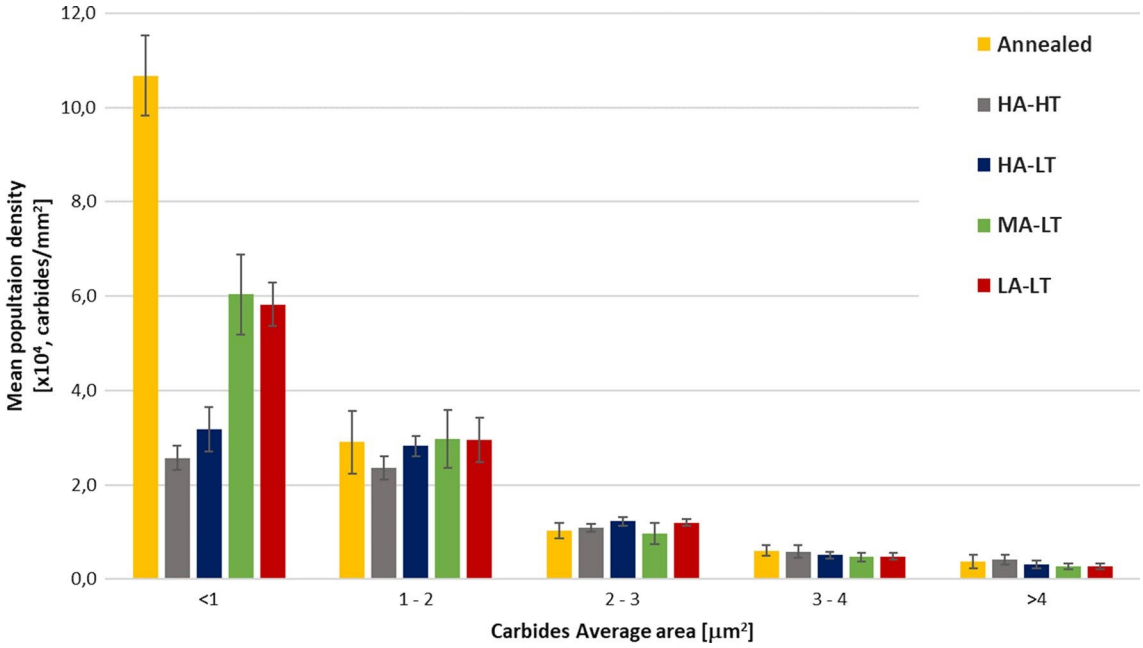

Fig. 4 Image analysis results of mean population density for average size of primary carbides

3.2 Retained Austenite and Hardness

XRD analyses were carried out to evaluate the amount of retained austenite in the investigated steel subjected to the different heat treatment conditions. Representative XRD patterns are reported in Fig. 5, and the main results are compared in Fig. 6 for the investigated treatment conditions. According to the microstructural analyses reported in Sect. 3.1, the γ(200) and γ(220) peaks, corresponding to the austenite phase, are more evident in the patterns of the HA-LT and MA-LT samples, while in the HA-HT and LA-LT ones, these are severally reduced and the martensite α(200) and α(211) peaks are instead prominent. According to the literature data [11,12], high tempering temperature over 400–450 °C promotes the complete transformation of RA, independently of the austenitizing condition. Figure 6 compares the effect of the different heat treatment parameters on both retained austenite and final hard- ness of the Q&T steel. The results highlight that under the same low tempering temperature conditions, the amount of RA is higher in the samples austenitized at high and medium temperatures, ranging from a maximum value of about 56 vol% in the HA-LT samples to about 4 vol% in the LA-LT samples. High tempering temperature promotes the almost complete transformation of the retained austenite pre- sent after quenching. In fact, by comparing HA-LT samples with HA-HT samples (same high temperature austenitizing), it can be observed that RA volume content decreases from about 56 vol% to about 4 vol%. A slight hardness increase is observed at higher austenitizing temperature. As observed in many studies [37,38], since a large amount of carbides solubilizes at high

austenitizing temperature, higher carbon content should be present in the martensitic laths. However, the hardness increase is not as high as expected because of the large content of retained austenite and typically macroscopic Rockwell C measurements integrate the response of a large microstructural volume which includes both martensite and RA. Similar results have been also reported in [38].

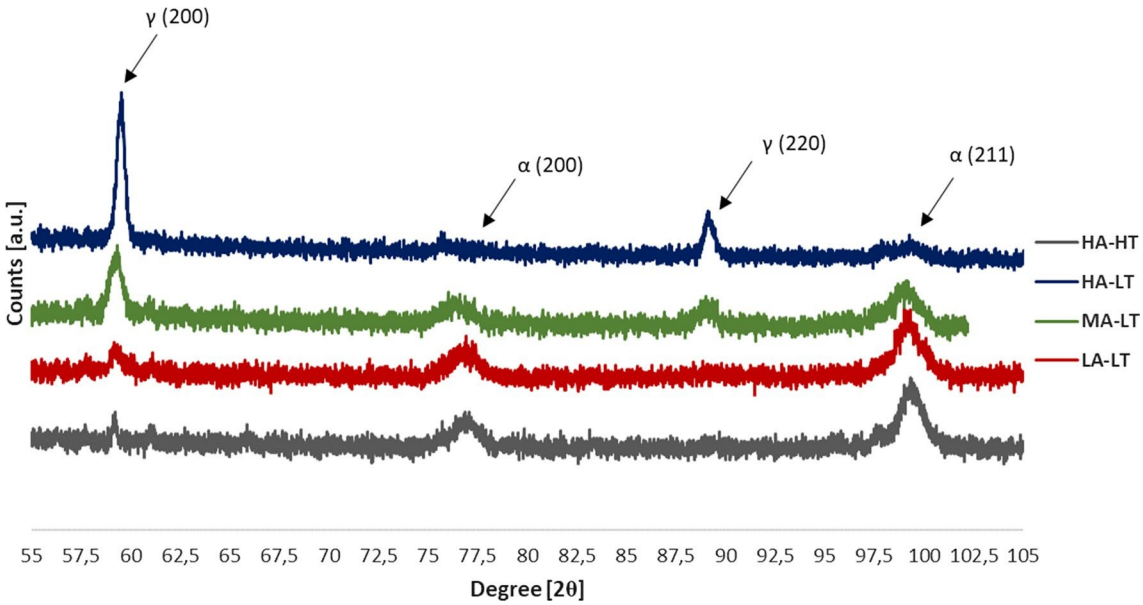

Fig. 5 XRD patterns for the determination of retained austenite content in samples with different heat treatment conditions

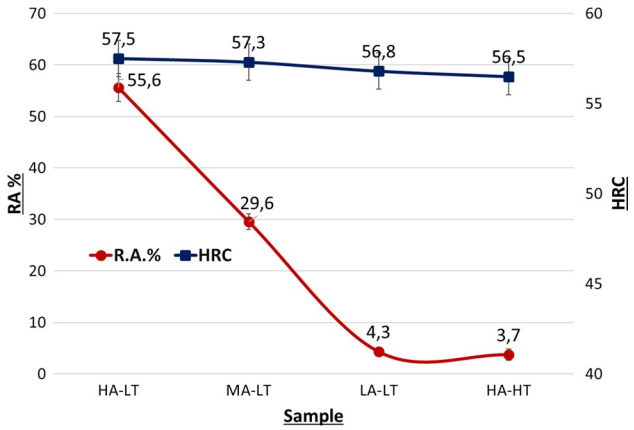

Fig. 6 Retained austenite and hardness curves corresponding to the different tested heat treatment conditions

3.3 Corrosion Resistance

The current potential curves after Q&T heat treatments are depicted in Fig. 7. All the samples show similar open cir- cuit potential values at OCP = − 0.47 V and all the recorded curves highlight the same features including two anodic peaks in the active area and then a current drop marking the begin of the passive area, as reported in literature [22, 26, 28]. In addition, for all the heat-treated samples, the break- down potentials recorded at the beginning of the transpassive However, differences in passivation current density (i_p) values of the heat-treated samples are clearly recorded. In the polarization curves reported in Fig. 7, passivation current density has been calculated as an average value of the pas- sive range plateau. In particular, the lowest i_p ($6.5.10^{-7}$ A/ cm^2) is measured for the HA-LT samples. Samples austen- itized in the range of temperatures of 1100–1120 °C and tempered at $T_{temp} < 350$ °C show higher current densities of 6.5×10^{-5} A/cm^2 and $1.2 \times$

10^{-4} A/cm^2 for MA-LT and LA-LT, respectively. For $T_{temp} > 450$ °C (HA-HT samples) current density increases rapidly ($i_p = 2.0 \times 10^{-3}$ A/cm^2), as reported in Fig. 7.

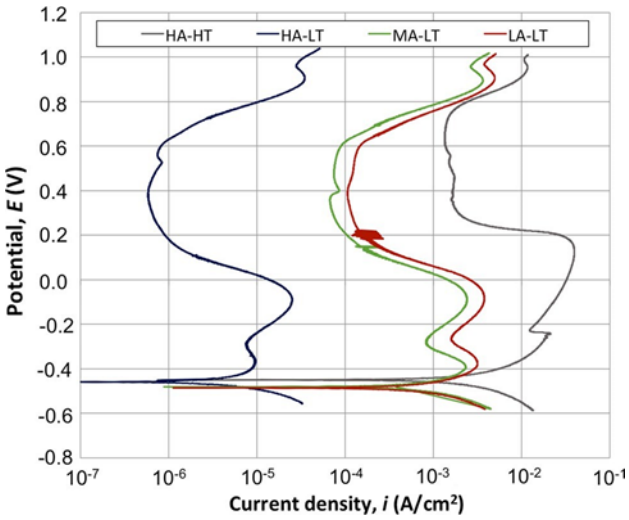

Fig. 7 Polarization curves recorded for the different heat-treated samples in 0.1 M H2SO4 solution

4 Discussion

4.1 Effect of Heat Treatment Conditions on Microstructure and Retained Austenite

The globular primary Cr-V carbides present in the annealed bar partially solubilize during austenitizing leading to a 25% amount reduction after high austenitizing temperature and 22% reduction after low austenitizing temperature (Fig. 3). As a consequence, samples austenitized at high temperature have a higher amount of carbon and alloying elements in the matrix respect to those austenitized at low temperature. It is widely known [2, 6, 14] that M_s and M_f temperatures lower if the contents of carbon and alloying elements increase in the austenite before quenching and this leads to higher amount of RA after quenching. This is in accordance with the result of the present study, since HA-LT and MA-LT samples have contents of RA one order of magnitude greater than LA-LT ones. Dissolution of carbides during austenitizing is also influenced by their size. Smallest carbides, in fact, give the greater contribution to the increase of carbon and alloying element in the austenite phase, and consequently to the presence of RA at room temperature. As reported in Sect. 3.1, dissolution of smaller carbides (in the range 0–1 μm^2) at high austenitizing temperature, in fact, represents about 75.5% in area of the total amount of dissolved carbides (Fig. 4). The largest carbides, instead, reduce their size and do not completely solubilize because of the lower surface area to volume ratio respect to the smaller ones, which reduce the rate of the diffusion processes. These larger carbides (> 4 μm^2) represent about 12.2% in area of the total amount of dissolved carbides. Therefore, finer the primary carbides, easier their dissolution, higher the content of carbon and alloying elements in the austenite before quenching, lower M_s and M_f and consequently higher the volume content of retained austenite. These results therefore suggest that the presence of RA after quenching is highly affected by the austenitizing temperature but that also by the size of primary carbides present in the starting annealed material. The large volume content of RA in HA-LT and MA-LT samples reduces the final hard- ness values of the heat-treated steels. From literature data [1,2,10,11] it is well known that tempering treatment mainly affects the amount of retained austenite. Tempering temperatures higher than 400–450 °C, in fact, are able to promote the transformation of the retained austenite into a martensite and secondary carbides structure [11, 12]. This statement is confirmed by the results of XRD analysis on HA-HT and HA-LT samples which underwent the same austenitizing condition but different tempering temperatures (Fig. 5). The low tempering temperature of the HA-LT treatment has not any substantial effect on the volume content of retained austenite, which is more than the 50%, while the higher temperature of the HA-HT leads to less than 4 vol% of RA (Fig. 6).

Precipitation of nano-sized Cr carbides, supposed to be formed after high tempering temperature [3, 21, 36] was not studied in the present investigation due to limited reso- lution of SEM and further studies are ongoing to evaluate this aspect

4.2 Effect of Q&T Conditions on Corrosion Resistance

The polarization E-i curves, reported in Fig. 7, highlight a strong influence of the heat treatment parameters (T_{aust} and T_{temp}) on the corrosion behaviour of X190CrVMo20-4-1 steel. In particular, the presence of RA in the lattice improves the corrosion resistance due to the fact that this phase contains lower internal stresses [23, 26], as high- lighted by low current density values of HA-LT and MA-LT samples characterised by an amount of RA of 55.6 vol% and 29.6 vol%, respectively. In particular, HA-LT sample shows the best corrosion resistance ($i_p = 6.5 \times 10^{-7}$ A/cm^2) thanks to a synergic beneficial effect of high amount of RA in the steel matrix as well as the highest dissolution of small Cr- rich carbides (< 1 μm^2), as depicted in Fig. 4. Increasing austenitizing temperature, lower current den- sities are recorded, as expected. This is mainly linked to the higher dissolution of Cr-rich carbides enhancing the Cr content in the matrix, as well as the increased amount of RA, as reported in [24, 25]. In addition, no strong differences in corrosion behaviour are shown between MA-LT and LA-LT samples. In particular, the beneficial effect of higher amount of RA in MA-LT than LA-LT (as reported in Fig. 7) leads to a slightly lower current density value. Tempering at high temperature (HA-HT) close to the second hardness peak impairs the corrosion resistance of the martensitic steel, as clearly highlighted by the polarization curves in which HA-HT sample exhibits the higher current density value (Fig. 7). This is due to the precipitation of nano-sized carbides (not investigated in this study) that induces a global Cr-depletion in the matrix as well as a local Cr-depletion due to the increased amount of carbides boundaries, as reported in literature studies [22, 26, 28, 29]. So low tempering temperature should always be preferred as clearly highlighted in the comparison between HA-LT and HA-HT that shows an improvement of current density of more than three orders of magnitudes. As proposed in [22, 28], due to the complex microstructure of the investigated samples, it is possible to identify three different activation peaks in the polarization curves recorded in H_2SO_4. In particular, $E_{p,1}$ is the passivation potential of the steel matrix far away from the carbides, $E_{p,2}$ is the passivation potential of the matrix close to the carbides and $E_{p,3}$ is the passivation potential of Cr-rich carbides [22, 28]. All the tested samples, except HA-HT, show the first activation peak around $E_{p,1} = -0.4$ V and a second activation peak around $E_{p,2} = -0.1$ V. Only HA-LT and MA-LT high- light an extra peak at around $E_{p,3} = 0.5$ V and 0.4 V, respec- tively. For HA-HT sample, the first activation is not clearly detectable, while $E_{p,2}$ shows the highest value of $E_{p,2} = 0.1$ V. In addition to the different current densities reported above, also $i_{p,1}$ (current density of the steel matrix far away from carbides) and $i_{p,2}$ (current density of the steel matrix close to carbides) show a trend in accordance with literature data [22, 28] for all the samples austenitized in the range of tempera- tures of 1100–1120 °C as $i_{p,2}$ increases rapidly compared to $i_{p,1}$, except for MA-LT sample that shows comparable values around 2.2×10^{-3} A/cm^2.Finally, the heat-treated sample by low T_{aust} and low T_{temp} shows good corrosion properties and low amount of RA in the matrix that theoretically reduces dimensional stability problems. So, it could state that these Q&T parameters allow a good compromise to have high hardness, good dimensional stability and good corrosion properties, necessary for the high-alloyed X190CrVMo20-4-1 tool stainless steel pro- duced with powder metallurgy (PM).

5 Conclusions

The aim of the present study was to understand the effect of principal heat treatment parameters on microstruc- ture and corrosion resistance of a high-alloyed tool steel X190CrVMo20-4-1 produced by powder metallurgy. Dif- ferent austenitizing and tempering temperatures have been analysed to correlate carbides distribution, dimensional sta- bility and corrosion resistance.The experimental results can be summarized as follows:

1. The austenitizing leads to a complete solubilization of small primary Cr-V carbides and a reduction in size of the biggest ones. Higher is the austenitizing temperature higher is the carbide solubilization.
2. During austenitizing, the elevated level of carbon and alloying elements in austenite solid solution reduces M_s and M_f characteristic temperatures and lead to a higher retained austenite content after quenching.
3. Tempering at low temperature does not have any effect on retained austenite while high tempering temperatures lead to the transformation of the main retained austenite percentage. The microstructure of HA-HT sample is predominantly martensitic.
4. Rockwell C hardness, which was supposed to increase with high austenitizing temperature, is instead strongly affected by the elevated amount of RA. The results do not show any significative variation in hardness.

5. The main parameters influencing corrosion resistance are the amount of RA in the matrix and tempering tem- perature. For this reason, high T_{aust} and low T_{temp} lead to
the best corrosion resistance. Moreover, tempering close
to the second hardness peak (HA-HT) is detrimental for corrosion resistance, so low tempering temperature should always be preferred as also lowers the internal stresses produced by quenching.
6. Finally, as high amount of RA in the matrix leads to dimensional stability problems, a good compromise between hardness and corrosion resistance properties is to apply low austenitizing and tempering temperatures. These parameters lead to low amount of RA (around 4 vol%) in the matrix, high hardness values (56.8 HRC) and good corrosion resistance (1.2×10^{-4} A/cm^2).

Acknowledgements The authors gratefully acknowledge SACMI IMOLA S.C. for the fruitful collaboration in the framework of scien- tific research on stainless steels.

References

1. K.E. Thelning, *Steel and Its Heat Treatment*, 2nd edn. (Butter- worths, London, 1984)
2. G.E. Totten, *Steel Heat Treatment Handbook*, 2nd edn. (CRC Press, Boca Raton, 2006)
3. T. Nykiel, T. Hryniewicz, Transformations of carbides during tempering of D3 tool steel. J. Mater. Eng. Perform. (2014). https ://doi.org/10.1007/s11665-014-0979-7
4. Y. Luo, H. Guo, X. Sun, M. Mao, J. Guo, Effects of austenitizing conditions on the microstructure of AISI M42 high-speed steel. Metals (Basel) **7**, 27 (2017). https://doi.org/10.3390/met7010027
5. R. Hossain, F. Pahlevani, V. Sahajwalla, Effect of small addi- tion of Cr on stability of retained austenite in high carbon steel. Mater. Charact. **125**, 114–122 (2017). https://doi.org/10.1016/j. matchar.2017.02.001
6. G. Roberts, G. Krauss, R. Kennedy, *Tool Steels*, 5th edn. (ASM International, Materials Park, 1998)
7. R. Hossain, F. Pahlevani, M.Z. Quadir, V. Sahajwalla, Stability of retained austenite in high carbon steel under compressive stress: an investigation from macro to nano scale. Sci. Rep. **6**, 34958 (2016). https://doi.org/10.1038/srep34958
8. D. Das, A.K. Dutta, K.K. Ray, Sub-zero treatments of AISI D2 steel: part I. Microstructure and hardness. Mater. Sci. Eng., A **527**, 2182–2193 (2010). https://doi.org/10.1016/j.msea.2009.10.070
9. Y.M. Rhyim, S.H. Han, Y.S. Na, J.H. Lee, Effect of deep cryo- genic treatment on carbide precipitation and mechanical proper- ties of tool steel. Solid State Phenom. **118**, 9–14 (2006). https:// doi.org/10.4028/www.scientific.net/SSP.118.9
10. S.-H. Yeh, L.-H. Chiu, Y.-T. Pan, S.-C. Lin, Relative dimen- sional change evaluation of vacuum heat-treated JIS SKD61hot-work tool steels. J. Mater. Eng. Perform. **23**, 2075–2082 (2014). https://doi.org/10.1007/s11665-014-0961-4
11. C.H. Surberg, P. Stratton, K. Lingenhöle, The effect of some heat treatment parameters on the dimensional stability of AISI D2. Cryogenics (Guildf) **48**, 42–47 (2008). https://doi. org/10.1016/j.cryogenics.2007.10.002
12. Y.-Y. Su, L.-H. Chiu, F.-S. Chen, S.-C. Lin, Y.-T. Pan, Residual stresses and dimensional changes related to the lattice parameter changes of heat-treated JIS SKD 11 tool steels. Mater. Trans. **55**, 831–837 (2014). https://doi.org/10.2320/matertrans.M2014
031
13. S. Kahrobaee, M. Kashefi, Microstructural characterization of quenched AISI D2 tool steel using magnetic/electromagnetic nondestructive techniques. IEEE Trans. Magn. **51**, 1–7 (2015). https://doi.org/10.1109/TMAG.2015.2428673
14. M. Kashefi, S. Kahrobaee, Determination of martensite start temperature using an electromagnetic nondestructive tech- nology. J. Alloys Compd. **720**, 478–482 (2017). https://doi. org/10.1016/J.JALLCOM.2017.05.283
15. M.T. Coll Ferrari, Effect of austenitising temperature and cool- ing rate on microstructures of hot-work tool steels (University West, 2015). ISBN 978-91-87531-16-3
16. L.D. Barlow, M. Du Toit, Effect of austenitizing heat treatment on the microstructure and hardness of martensitic stainless steel AISI 420. J. Mater. Eng. Perform. **21**, 1327–1336 (2012). https
://doi.org/10.1007/s11665-011-0043-9
17. I. Gunes, M. Uzun, A. Cetin, K. Aslantas, A. Cicek, Evaluation of wear performance of cryogenically treated Vanadis 4 Extra tool steel. Kovove Mater. **54**(3), 195–204 (2016). https://doi. org/10.4149/km20163195
18. D.N. Collins, J. Dormer, Cryogenic treatment deep cryogenic treatment of a D2 cold-work tool steel. Int. Heat Treat. Surf. Eng. **2**(3–4), 150–154 (2008). https://doi.org/10.1179/17495 1508X446376
19. F. Meng, K. Tagashira, R. Azuma, H. Sohma, Role of eta- carbide precipitations in the wear resistance improvements of Fe-12Cr-Mo-V-1.4C tool steel by cryogenic treatment. ISIJ Int. **34**, 205–210 (1994). https://doi.org/10.2355/isijinternation al.34.205
20. A. Chatterjee, M. Faktor, R. Moss, E. White, A simplified tech- nique for MOCVD of III–IV compounds. J. Phys. Colloq. **43**(C5), 491–503 (1982). https://doi.org/10.1051/jphyscol:1982560
21. S.-Y. Lu, K.-F. Yao, Y.-B. Chen, M.-H. Wang, X. Liu, X. Ge,
The effect of tempering temperature on the microstructure and electrochemical properties of a 13 wt% Cr-type martensitic stain- less steel. Electrochim. Acta **165**, 45–55 (2015). https://doi. org/10.1016/j.electacta.2015.02.038

22. M. Seifert, D. Wieskämper, T. Tonfeld, S. Huth, Corrosion proper- ties of a complex multi-phase martensitic stainless steel depend- ing on the tempering temperature. Mater. Corros. **66**, 1290–1298 (2015). https://doi.org/10.1002/maco.201508229
23. H. Hill, S. Huth, S. Weber, W. Theisen, Corrosion properties of a plastic mould steel with special focus on the processing route. Mater. Corros. **62**, 436–443 (2011). https://doi.org/10.1002/ maco.200905570
24. A.F. Candelária, C.E. Pinedo, Influence of the heat treatment on the corrosion resistance of the martensitic stainless steel type AISI 420. J. Mater. Sci. Lett. **22**, 1151–1153 (2003)
25. Y.-S. Choi, J.-G. Kim, Y.-S. Park, J.-Y. Park, Austenitizing treatment influence on the electrochemical corrosion behavior of 0.3C–14Cr–3Mo martensitic stainless steel. Mater. Lett. **61**, 244–247 (2007). https://doi.org/10.1016/j.matlet.2006.04.041
26. H. Hill, U. Raab, S. Weber, W. Theisen, M. Wollmann, L. Wagner, Influence of heat treatment on the performance characteristics of a plastic mold steel. Steel Res. Int. **82**, 1290–1296 (2011). https://doi.org/10.1002/srin.201100098
27. O.N. Mohanty, On the stabilization of retained austenite: mecha- nism and kinetics. Mater. Sci. Eng., B **32**, 267–278 (1995). https://doi.org/10.1016/0921-5107(95)03017-4
28. S. Huth, H. Hill, W. Theisen, Corrosion of stainless PM tool steels: interpretation of current density potential curves in acid environments. HTM J. Heat Treat. Mater. **65**, 195–200 (2010). https://doi.org/10.3139/105.110067
29. S. Peissl, G. Mori, H. Leitner, R. Ebner, S. Eglsäer, Influence of chromium, molybdenum and cobalt on the corrosion behaviour of high carbon steels in dependence of heat treatment. Mater. Corros. **57**, 759–765 (2006). https://doi.org/10.1002/maco.200503969
30. A.N. Isfahany, H. Saghafian, G. Borhani, The effect of heat treat- ment on mechanical properties and corrosion behavior of AISI420 martensitic stainless steel. J. Alloys Compd. **509**, 3931–3936 (2011). https://doi.org/10.1016/J.JALLCOM.2010.12.174
31. ASTM E975-13, *Standard Practice for X-Ray Determination of Retained Austenite in Steel with Near RandomCrystallographic Orientation* (ASTM International Standards Organization, West Conshohocken, 2013)
32. EN ISO 6507-1:2018, Metallic Materials—Vickers Hardness— Part 1: Test Method (CEN-CENELEC, Brussels, 2018)
33. ASTM A892-09, *Standard Guide for Defining and Rating the Microstructure of High Carbon Bearing Steels* (ASTM Interna- tional, West Conshohocken, 2009)K. Fukaura, Y. Yokoyama, D. Yokoi, N. Tsujii, K. Ono, Fatigue of cold-work tool steels: effect of heat treatment and carbide morphology on fatigue crack formation, life, and fracture surface observations. Metall. Mater. Trans. A **35**, 1289–1300 (2004). https://doi.org/10.1007/s11661-004-0303-5
34. ASTM G5–14, *Standard Reference Test Method for Making Poten- tiodynamic Anodic Polarization Measurements* (ASTM Interna- tional Standards Organization, West Conshohocken, 2014)
35. G. Chakraborty, C.R. Das, S.K. Albert, A.K. Bhaduri, V. Thomas Paul, G. Panneerselvam, A. Dasgupta, Study on tempering behav- iour of AISI 410 stainless steel. Mater. Charact. **100**, 81–87 (2015). https://doi.org/10.1016/j.matchar.2014.12.015
36. M. Yaso, S. Morito, T. Ohba, K. Kubota, Microstructure of mar- tensite in Fe–C–Cr steel. Mater. Sci. Eng., A **481–482**, 770–773 (2008). https://doi.org/10.1016/J.MSEA.2007.03.114
37. G. Krauss, Martensite in steel: strength and structure. Mater. Sci. Eng., A **273–275**, 40–57 (1999). https://doi.org/10.1016/S0921-5093(99)00288-9